Abdelhamid Henchiri[1,*], Tahar Bahi[2], Moufid Mohammedi[3], Amira Lakhdara[3].

J. Electrical Systems 20-2 (2024): 142-156

Regular paper

Energy Management and Control of Multi - Source System

Journal of Electrical Systems

The utilization of renewable energy sources is on the rise and will have a significant impact on future energy grids. This paper focuses on developing management systems for grid-connected systems incorporating solar photovoltaic panels and batteries, taking into account varying radiation levels and operational scenarios. The management of the energy storage system linked to the grid involves regulating battery charge, discharge, and hold operations using a bidirectional DC-DC converter tailored to meet load requirements. The performance of the grid-connected system with solar PV and battery is assessed, employing a maximum power point tracking algorithm to optimize voltage levels continuously. Additionally, a lithium-ion battery-based storage system is integrated with the PV setup, which includes an MPPT controller and boost converter for enhanced efficiency.

Keywords: Renewable energy, Photovoltaic system; battery storage; Energy management; simulation.

1. Introduction

The transition towards a sustainable energy future has become a global priority, driven by the need to reduce greenhouse gas emissions and minimize our reliance on fossil fuels. Renewable energies (RE), such as solar, wind, hydroelectricity, biomass, and other sources, offer considerable potential to meet our energy needs while reducing our environmental footprint [1,2]. Indeed, the development of renewable energy-based installations emerges as a promising solution to ensure a transition towards a cleaner and more sustainable energy future. Their use holds significant interest at multiple levels, as well as challenges to overcome in order to maximize their adoption and efficiency. Furthermore, their diversity enables a more decentralized approach to energy production, providing greater autonomy to communities and reducing dependence on centralized energy infrastructure [3]. However, renewable energy sources (RES), such as solar and wind, are intermittent and reliant on weather conditions. This poses challenges in ensuring stable and reliable energy supply, necessitating investments in energy storage, smart grids, and other intermittency management technologies [4, 5]. Therefore, by overcoming these challenges and capitalizing on the advantages of renewable energies, we can accelerate the transition towards a more sustainable, resilient, and equitable energy system.

Regarding the use of solar energy as the main source in the installation considered in this work, the intermittency of solar energy stands out as one of the primary challenges to overcome [6,7]. Indeed, the availability of solar energy heavily relies on weather conditions and day-night cycles. Therefore, to ensure continuity of service and meet energy demand even when solar production is limited, the installation of energy storage systems becomes

* Corresponding author[1]: A. Henchiri, Laboratory of Mechanical Engineering and Materials, 20 August 1955-Skikda University, Skikda 21000, Algeria, E-mail: a.henchiri@univ-skikda.dz
[2] Automatic Laboratory and Signals LASA Badji Mokhtar University, Annaba, 2300, Algeria
[3] Badji Mokhtar University, Annaba, 2300, Algeria

essential. These systems enable the capture of excess energy produced during periods of high solar irradiation and store it in the form of electricity. Subsequently, this stored energy can be used to meet demand during periods of low solar production, thereby ensuring a more reliable energy supply .The stored energy can be utilized to power electrical grids or meet demand during periods of low solar production, ensuring a stable and reliable power supply. These storage installations also present a challenge to overcome, as they require managing power flows within different parts of the photovoltaic installation. Installing storage systems thus helps mitigate the impact of solar energy intermittency, enhancing the reliability of the electrical grid and accelerating the transition towards cleaner and more sustainable energy.

Photovoltaic installations connected to a single-phase electrical grid, equipped with storage batteries, represent an innovative and efficient solution for maximizing the use of solar energy and ensuring a reliable and stable power supply [8-10]. The functioning principle of these installations relies on harnessing solar energy through photovoltaic panels (PV) that convert sunlight into direct current electricity [11]. This direct current electricity is then converted into alternating current by an inverter, thus adapting solar production to the needs of the domestic electrical grid. Batteries allow for the storage of excess electricity produced during periods of high solar irradiation, for later use when solar production is reduced or when energy demand is high. Thus, the batteries act as a buffer, ensuring a continuous and stable power supply even when weather conditions are not conducive to solar production. This work focuses on the control and management of power flows in a multi-source installation within this framework. This installation primarily consists of a photovoltaic generator (PVG) connected to a single-phase electrical grid and equipped with a storage battery. The entire system powers a load with direct current.

The objective of this work is to study energy management in the photovoltaic system connected to the grid with the maximum power point tracking (MPPT) controller, and to control and manage power flows between the photovoltaic source, the electrical grid, storage batteries, and the load. Furthermore, it aims to evaluate the operational performance of the entire multi-source system under variable irradiation profiles using MatLab/Simulink software.

The structure of this paper is outlined as follows: In the second section, the configuration of the system is introduced, along with the modelling of its diverse components such as the solar panel, boost converters, buck-boost converters, and storage batteries. The third section presents the development of an optimization algorithm based on fuzzy logic, designed to track the instantaneous maximum power generated by the photovoltaic system. A numerical simulation is detailed in the fourth section to scrutinize and validate the functionality of the entire system across different irradiation profiles. Lastly, the conclusion encapsulates the essential findings and contributions of this study.

2. System description and modelling

The proposed system for this study is depicted in Figure 1. It primarily consists of a continuous load connected to the DC bus, to which a photovoltaic generator (GPV) is also connected. The PV array converts solar energy into direct current electricity. The energy produced by the PV array is supplied to the load through a Boost converter controlled by a Maximum Power Point Tracking (MPPT) algorithm. This MPPT algorithm dynamically adjusts the converter's parameters in real-time to operate the system at the maximum power point, ensuring enhanced conversion efficiency.

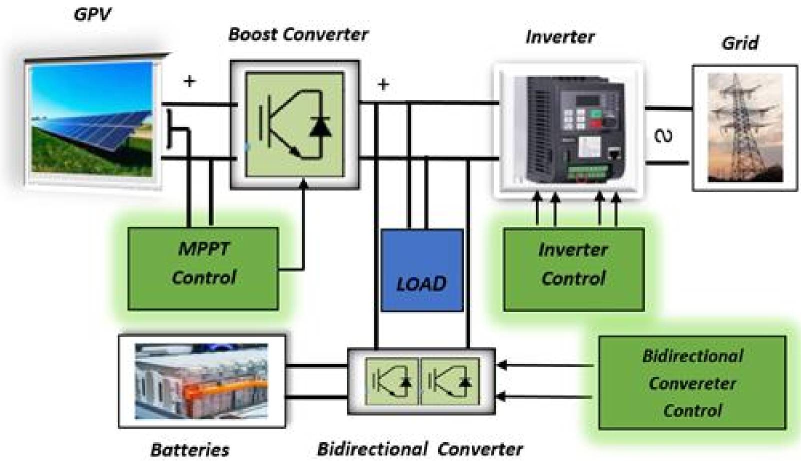

Fig. 1. System description block diagram

The bus to which the load is connected serves as the crucial link between the different sources of the multisource system: the renewable energy source, the electrical grid, and the storage system. This necessitates efficient management to maintain stability and quality of power supply. Simultaneously, a single-phase grid with power control and management is integrated to ensure smooth distribution of electricity to the continuous load. This control adapts the delivered power according to the load requirements and fluctuations in solar production, ensuring a consistent and tailored power supply. Finally, a storage system comprising batteries, powered by a reversible converter, is included to ensure energy availability even when solar production is insufficient or absent. This system stores excess energy during periods of high solar production and releases it as needed to meet the demand of the continuous load, thus ensuring uninterrupted and reliable power supply.

3. System modelisation

3.1. *Modelling and characteristics of the photovoltaic system*

The single-diode model depicted in Figure 2 is one of the simplest and commonly used models to represent the electrical behaviour of a photovoltaic cell. The photovoltaic cell is represented as an ideal current source (I_{ph}) in series with a diode (D), and a parallel resistance (R_p) represents the loss due to the low leakage current flowing through the parallel path. Additionally, a series resistance (R_s) represents the losses, which include grid metallic loss, contacts, and current collection bus. The diode represents the process of converting solar light into electrical current [12, 13].

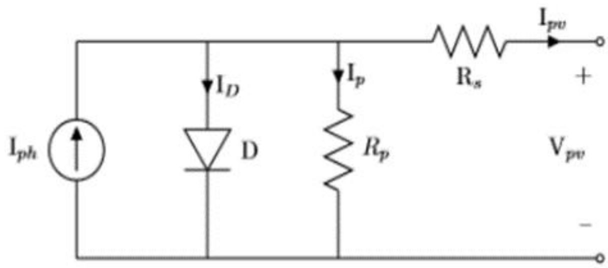

Fig. 2. Single diode Model

The open-circuit voltage (V_{oc}) and short-circuit current (I_{sc}) of the cell are key parameters used to determine the characteristics of the diode in the model. From these parameters, the current-voltage relationship of the diode can be determined using the following diode equations, which enable predicting the cell's behaviour under different solar irradiance and temperature conditions [14-16].

$$I_{out} = I_{sc} - I_D \tag{1}$$

$$I_D = I_o.(e^{q(V+R_sI)/nKT} - 1) \tag{2}$$

$$I_{out} = I_L - I_o.(e^{q(V+R_sI)/nKT} - 1) - (V + R_sI)/R_p \tag{3}$$

I_L is the current of photovoltaic array; Io represents the PV array reverse saturated current, q means the electron charge K is the Boltzmann constant (1, 38.10^{-23} J/K) and T is the temperature of the p-n junction.

The critical process in identifying the maximum power point of a PV panel involves determining the Current -Voltage (I=f (V)) and Power -Voltage (P=f (V)) characteristic curves of the panel. Higher irradiation levels result in elevated power and voltage outputs from the PV panel, whereas rising temperatures exert a detrimental effect on both power and voltage. The data of the photovoltaic system considered in this work are listed in Table 1. Figures 3 (a, b,) and Figures 4 (a, b,) depict the P=f(V) and I=f(V) characteristic curves, respectively, under varying irradiance and temperature conditions. Then afterward, Table 2 presents the characteristic point values for different irradiation and temperature values.

Table 1: Data of the photovoltaic system

Maximum Power (w)	258.25
Cells per Modul (Ncell)	60
Open Circuit Voltage Voc(V)	37.3
Short –Circuit Current Isc(A)	8.66
Voltage at Maximum Power Point Vmp(V)	30.7
Current at Maximum Power Point Imp(V)	8.15
Parallel Stings	1
Series- Connected Modules per String	8

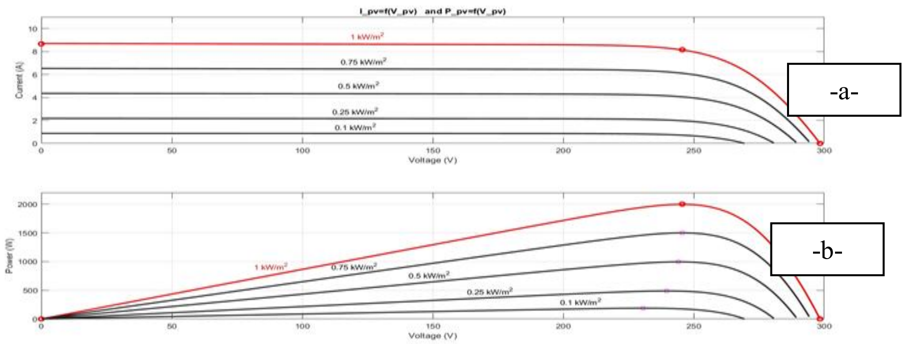

Fig. 3. I_{pv}=f(V_{pv}) and P_{pv}=f(V_{pv}) where E=variable and T=Cont=25°C

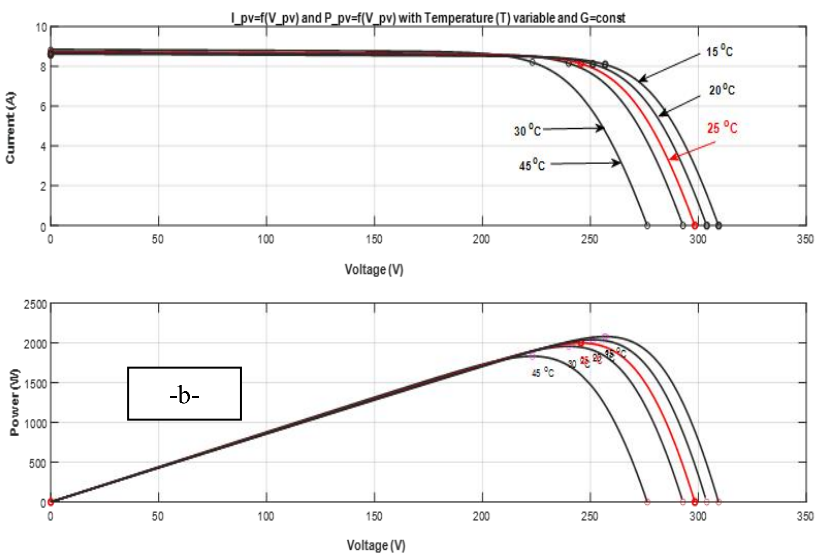

Fig. 4. I_{pv}=f(V_{pv}) and P_{pv}=f(V_{pv}) when E=variable and T=Cont=25°C

Table 2: Characteristic point values when E= Const=1Kw/m^2 and T=variable.

E(Kw/m^2)		1	0.75	0.5	0.25	0.1
T=25°C	P_{pv_max}	2001	1500	995.2	448	230.6
	V_{pv_max}	245.6	245.3	244.1	239.6	187.85
	I_{cc_max}	8.66	6.52	4.35	2.17	0.87

Table 3: Characteristic point values for E= Const=1Kw/m^2 and T=variable.

T(°C)		15	20	25	30	45
E=1Kw/m^2	P_{pv}_max	2078.34	2038	2001	1956.3	18.67
	V_{pv}_max	256.85	251	245.6	239.95	218.95
	I_{cc}_max	8.09	8.11	8.66	8.10	8.20

3.2. *Modelling of the Boost converter*

The Boost converter is installed to increase the photovoltaic array voltage to a level, which ensures correct operation of the inverter and he controlled by the duty ratio (α) with which the average values of the output quantities can be expressed with those of the input [17,18]. Electrical circuit is illustrated in Figure 5.

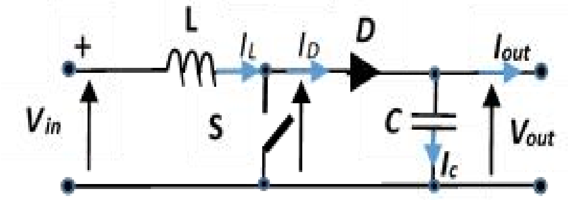

Fig. 5. Electrical circuit of the Boost converter

The semiconductor (S) is used as a switch and it is in "open" or "closed" states. Thus, in terms of modeling this converter, when we assume that all components are ireal [19], Thus, in terms of modeling this converter, two operating modes are distinguished, and consequently, two possible configurations exist depending on whether S=open or S=closed. The corresponding electrical circuits for these states are depicted in Figures 6 and 7, respectively.

• When S is closed:

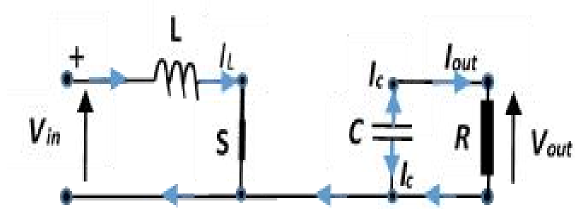

Fig. 6. Electrical Circuit when S is closed

During this cycle (αT), the current through the inductance increases gradually and L stores energy.

So, the state equations are:

Where I_L denotes the current of inductor and V_c denotes the voltage of capacitor.

• When S is opened:

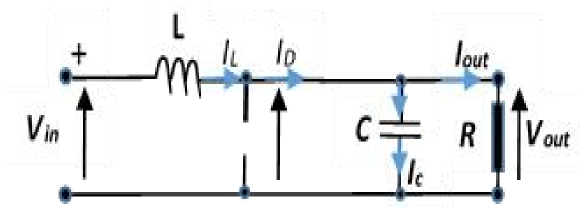

Fig. 7. Electrical Circuit when S is opened

During this cycle (T (1-αT)), the inductance (L) opposing the current decrease increases gradually and L stores energy. , generates a voltage which is added to source voltage which is applied to the load (R) through the diode (D).

So, the state equations are:

$$\begin{bmatrix} \dot{x_1} \\ \dot{x_2} \end{bmatrix} = \begin{bmatrix} 0 & \frac{-1}{L} \\ \frac{1}{C} & \frac{-1}{RC} \end{bmatrix} \begin{bmatrix} x_1 \\ x_2 \end{bmatrix} + \begin{bmatrix} \frac{1}{L} \\ 0 \end{bmatrix} \begin{bmatrix} x_1 \\ x_2 \end{bmatrix} V_{in} \tag{5}$$

Considering the current of the inductor (I_L) and the voltage of the capacitor (V_c) as state variables designated respectively as x_1 and x_2, we derive the two corresponding state-space representations for the two operating modes, as follows:

$$\begin{bmatrix} \dot{x_1} \\ \dot{x_2} \end{bmatrix} = \begin{bmatrix} 0 & 0 \\ 0 & \frac{-1}{RC} \end{bmatrix} \begin{bmatrix} x_1 \\ x_2 \end{bmatrix} + \begin{bmatrix} \frac{1}{L} \\ 0 \end{bmatrix} \begin{bmatrix} x_1 \\ x_2 \end{bmatrix} V_{in} \tag{4}$$

Based on the previous representations, we get the average model of the boost converter.

$$\begin{bmatrix} \dot{x_1} \\ \dot{x_2} \end{bmatrix} = \begin{bmatrix} 0 & \frac{\alpha-1}{L} \\ \frac{1-\alpha}{C} & \frac{-1}{RC} \end{bmatrix} \begin{bmatrix} x_1 \\ x_2 \end{bmatrix} + \begin{bmatrix} \frac{1}{L} \\ 0 \end{bmatrix} V_{in} \tag{6}$$

3.3. B*uck-Boost modelling*

A Buck-Boost converter integrates the operating principles of both the Buck Converter and the Boost Converter into a unified circuit, functioning as a switched mode power supply [20-21]. Fortunately, these both converters use very similar components. An additional control unit is incorporated into the system, which detects the input voltage level and subsequently determines the suitable course of action for the circuit. The corresponding electrical circuit is shown in Figure 8.

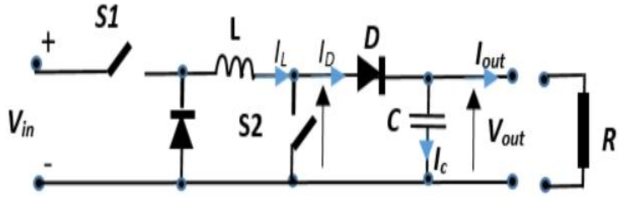

Fig. 8. Electrical Circuit of Buck-Boost converter

In this setup, both switches operate in unison, meaning they are either both closed or both open. During the period when the switches are open, the inductor's current gradually builds up. When the switches reach a suitable point, they are opened, allowing the inductor to discharge and supply current to the load through a path incorporating both diodes, D1 and D2. Hence, we derive the mathematical expressions relating to the states of the two semiconductors S1 and S2, as follows [22, 23]: If the duty cycles of the PWM signals controlling S1 and S2 are denoted by α1 and α2 respectively, then the output DC voltage V_o can be expressed by the following equation:

$$\frac{V_o}{V_{in}} = \frac{\alpha_1}{1-\alpha_2} \tag{7}$$

When $\alpha_1 + \alpha_2 > 1$: Step Up and if $\alpha_1 + \alpha_2 < 1$: Step Down

In the buck-boost operation mode, when S2 turns on while S1 is off, there's a risk of shorting the inductance through diode D1, potentially damaging either the diode or the inductance due to the resulting short circuit current. To prevent this scenario, it's crucial that the diode D2 be consistently smaller than diode D1. Specifically, S2 should only receive the switching signal when S1 is on. The spatial model is derived as follows:

$$\begin{bmatrix} \dot{x}_1 \\ \dot{x}_2 \end{bmatrix} = \begin{bmatrix} -\frac{1-\alpha 2}{L} & 0 \\ -\frac{1}{RC} & \frac{1-\alpha_2}{C} \end{bmatrix} \begin{bmatrix} x_1 \\ x_2 \end{bmatrix} + \begin{bmatrix} \frac{\alpha_1}{L} \\ 0 \end{bmatrix} Vi_n \tag{8}$$

3.4 *Modelling of Battery Storage System*

The battery model represented by the circuit diagram in Figure 9 consists of a DC voltage (E) and a constant internal resistance (R_{int}), which require only two measurements to practically determine their values. This model utilizes only the State of Charge (SOC) as the state variable [24-26]. The voltage is modeled by a controlled voltage source dependent on the SOC, as shown in equations (9) and (10). The explanation of the variables in the following equations and circuit diagrams is available.

$$E = E_0 - K\frac{Q_0}{Q_0 - Q}Ae^{-BQ} \tag{9}$$

Where,

$$Q = \int_0^t - I_{bat}dt \tag{10}$$

The variable Q denotes the current battery charge, while Q0 represents the rated battery capacity. The state of charge (SOC) is calculated as the ratio Q/Q0. To model the actual battery charge, the battery current is integrated, and the initial charge is added, as illustrated in the equation depicted in the figure below.

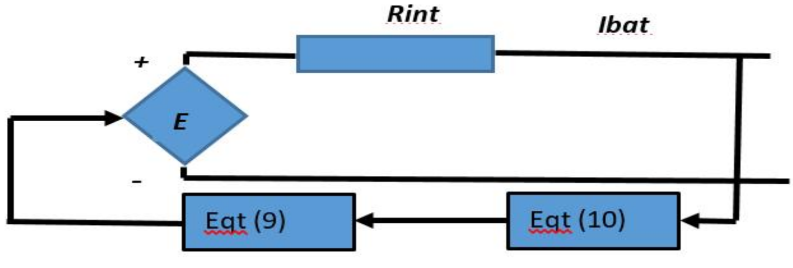

Fig. 9. Circuit diagram of battery

A typical discharge curve consists of three distinct sections, as depicted in the figure 10. The initial section illustrates the exponential voltage decline during the battery's charging phase, with the width varying depending on the battery type. The second section signifies the usable charge available from the battery until the voltage falls below the nominal voltage level. Finally, the third section depicts the complete discharge of the battery, characterized by a rapid voltage drop. In cases where the battery current is negative, indicating charging, the battery follows a charging characteristic as illustrated in the figure below. During charging, the voltage exponentially increases, regardless of the battery's state of charge (SOC). Conversely, during discharging, the exponential voltage decline is immediate.

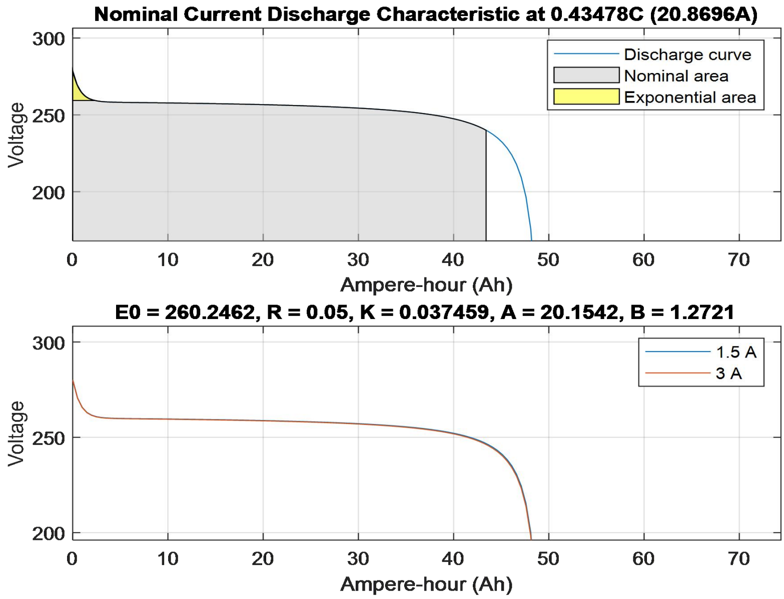

Fig. 10. Discharge Characteristics

4. MPPT Control

Control of the boost converter for maximum power point tracking (MPPT) is a crucial method for optimizing the efficiency of photovoltaic systems. This control dynamically adjusts converter parameters to maintain voltage or current at an optimal level for extracting maximum power from the solar panel under varying irradiation and temperature conditions. Classical MPPT techniques such as Perturb and Observe (P&O) and Incremental Conductance (IncCond) are widely used for their simplicity and effectiveness under standard operating conditions. Conversely, advanced approaches like genetic algorithms and artificial neural networks offer finer optimization and dynamic adaptation to environmental variations, enhancing photovoltaic system performance in variable and complex conditions [27-28].

In this study, an intelligent MPPT control based on fuzzy logic (FL) is utilized due to its ability to effectively handle imprecise, uncertain, and ambiguous data without requiring precise mathematical modeling of the system. The FL system comprises three sequential blocks: fuzzification, inference, and defuzzification, as depicted in Figure 11.

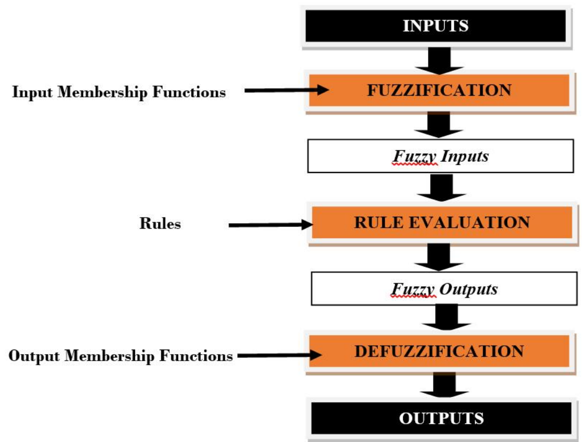

Fig. 11. Fuzzy logic structure

During the fuzzification process, measured input variables are transformed into fuzzy variables using predefined membership functions. The inference phase facilitates the transition from fuzzy input variables to fuzzy output variables through the application of "IF-THEN" rules and inference techniques. These rules establish a linguistic link between input and output variables, crafted based on human understanding of the process [29-30]. In the final step, known as defuzzification, the fuzzy output set is translated into a precise numerical value to execute the desired system behavior accurately. The rule base table stands as the cornerstone of the FLC, tailored to the specific application and informed by prior knowledge.

This strategy, specifically designed for controlling the Boost converter, enables the optimization of the system's energy efficiency by maximizing the conversion of electrical energy from sunlight while efficiently utilizing available resources. To achieve this goal, the MPPT employing Fuzzy Logic has been implemented to regulate the Boost converter. This control scheme utilizes input variables (V_{pv}, P_{pv}), and the Fuzzy Logic Controller leverages information about E(k) and ΔE(k) to determine the appropriate duty cycle (α) value [31-32].

$$E(k) = \frac{\Delta P(k)}{\Delta V(k)} = \frac{P(k)-P(k-1)}{V(k)-V(k-1)} \tag{11}$$

$$\Delta E(k) = E(k) - E(k-1) \tag{12}$$

The fuzzification process converts the previous numerical input variables (E(k) and ΔE(k)) into linguistic variables which can take the following five values : NB (Negative Big), NS (Negative Small), ZE (Zero), PS (Positive Small), PB (Positive Big). According to the evolution of the input parameters and the rules base given in Table 4.

Table 4 : Rules tables

:::::	NB	NS	EZ	PS	PB
NB	ZE	ZE	NS	PS	PB
NS	ZE	ZE	ZE	PS	PB
EZ	NB	NS	ZE	PS	PB
PS	NB	NS	ZE	ZE	ZE
PB	NB	NS	PS	ZE	ZE

5. Simulation results

Let us recall that we previously emphasized that the impact of irradiation variation is significantly more significant than that of temperature on the behavior of the photovoltaic system. In our experiments, we therefore assume that the temperature remains constant and propose a profile of irradiation variation, as illustrated in Figure 12.

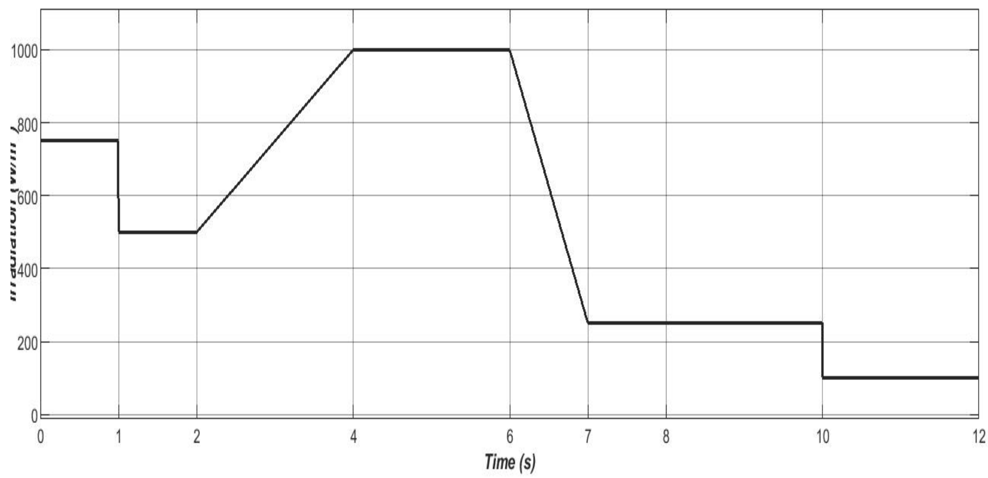

Fig. 12. Profil of irradiation

Under the influence of this profile and in these conditions, we analyzed and evaluated the operational performance of the system. As can be observed, the irradiation profile is divided into seven (7) distinct intervals where the irradiation level varies either instantaneously or progressively (2s ≤ time ≤ 4s and 6s ≤ time ≤ 7s). Figure 13 illustrates voltage variations. Figure 13a depicts the voltages across the photovoltaic panel, the load, and the storage batteries. Figure 13b shows the duty cycles applied to the Boost converter and the reversible Buck-Boost converter. Lastly, Figure 13c displays the power produced by the photovoltaic panel, the power consumed by the load, and the power stored or supplied by the batteries. Figure 13d visualizes the state of charge (SOC), enabling us to determine whether the storage system operates in charge or discharge mode. By analyzing the powers (Figure 13c) and the SOC (Figure 13d), we can establish correspondence with the specifications outlined in the project requirements. Figure 14 illustrates the sinusoidal voltage of the electrical grid overlaid with the grid current and that of the inverter after filtering. It is worth noting that these currents have been multiplied by fifty (*50) for better clarity. Figure 14b represents the currents at the DC bus of the photovoltaic system, as well as those of the load, the batteries, and the inverter, with the sum of all currents shown at the bottom. We observe that they vary according to the irradiation profile imposed for the test.

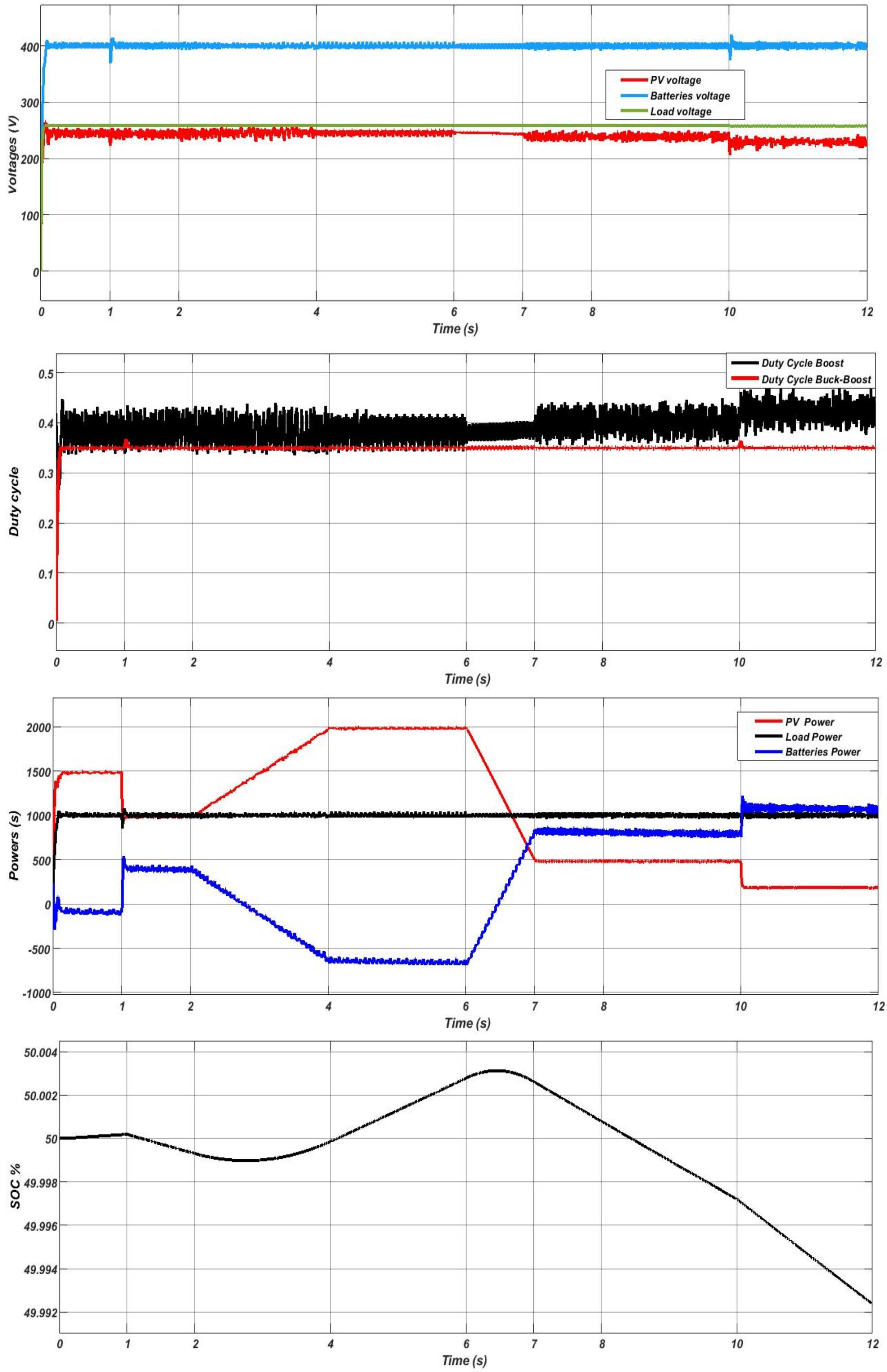

Fig. 13. Voltages, Duty cycle, Powers and SOC

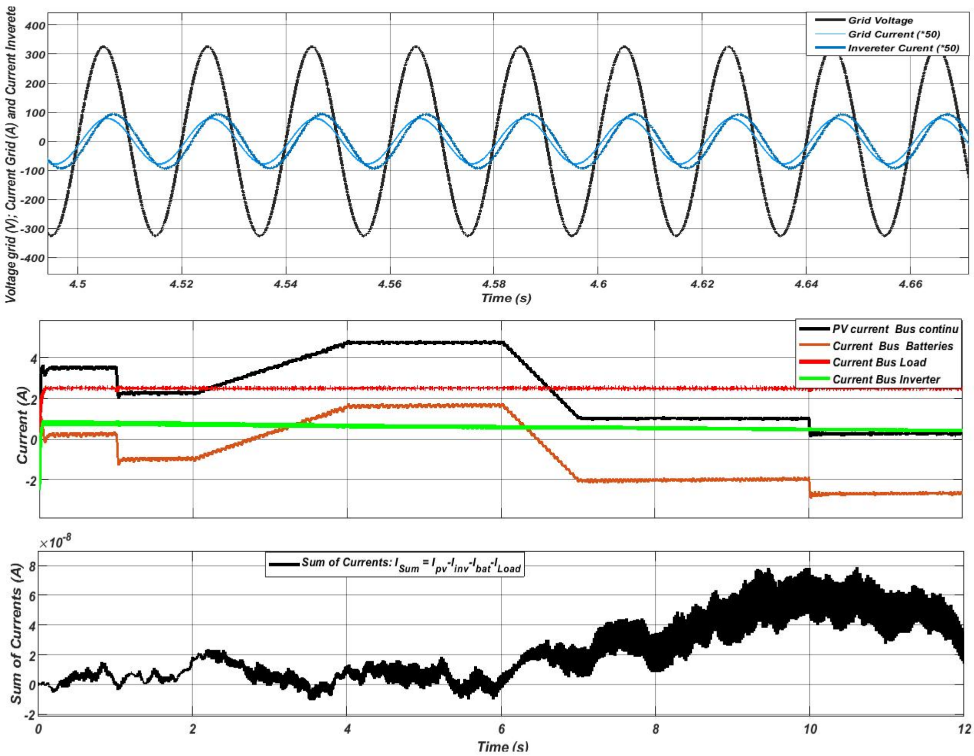

Fig. 14. Voltage grid and Currents

6. Conclusion

The multi-source system studied in this research primarily consists of a photovoltaic system as the main energy production source, a battery-based storage system as an auxiliary source to ensure service continuity during unfavorable weather conditions, and a load connected to the DC bus, which is in turn connected to a single-phase electrical grid. Regarding the contribution of optimization algorithms for controlling the boost converter directly associated with the photovoltaic system, an intelligent technique based on fuzzy logic has been adapted for controlling the reversible converter intended for charging and discharging the storage system. By subjecting the entire system to the effect of an irradiation profile consisting of various levels and types of evolutions, thus reflecting a model closer to reality, the analysis of different parameters, including voltages, currents, powers, and battery state of charge, has demonstrated that the system operates correctly according to the desired operating principle. Multi-source systems offer a versatile and efficient solution to address diverse and complex energy needs. Their ability to integrate multiple energy sources, such as solar and batteries, allows for better reliability and optimal use of available resources. Additionally, these systems promote energy resilience by reducing dependence on a single source while contributing to the transition toward a more sustainable and eco-friendly energy infrastructure. Their increased flexibility also provides advantages in terms of adaptability to demand variations and environmental conditions, thereby reinforcing the stability and efficiency of electrical grids. In summary, multi-source systems represent a promising innovation for addressing current challenges in energy management while laying the groundwork for a more resilient and sustainable energy future.

References

[1] Saptaparna Basu Roy Chowdhury , P. K. Gayen , Saptarshi Roy , N V Phanendra Babu, A Novel MPPT algorithm for PV systems under variable Shading Conditions using Horse Herd Optimization, *J. Electrical Systems JES*, 18-1 , 82-96, 2022.

[2] A. Qazi et al. Towards Sustainable Energy: A Systematic Review of Renewable Energy Sources, Technologies, and Public Opinions, *in IEEE Access*, vol. 7, pp. 63837-63851, 2019, doi: 10.1109/ACCESS.2019.2906402.

[3] A Lakhdara, T Bahi, A Moussaoui , "Energy Management and Control of a Photovoltaic System Connected to the Electrical Network," 2020 17th International Multi-Conference on Systems, Signals & Devices (SSD), Monastir, Tunisia, 2020, pp. 65-72, doi: 10.1109/SSD49366.2020.9364183.

[4] Han, Y.; Li, Q.; Wang, T.; Chen, W.; Ma, L. Multisource Coordination Energy Management Strategy Based on SOC Consensus for a PEMFC-Battery-Supercapacitor Hybrid Tramway. IEEE Trans. *Veh. Technol*. 67, 296–305, 2018.

[5] Suresh H, Baskaran A, Sudharsan KP, Vignesh U, Viveknath T, Sivraj P, Vijith K, Amrita Vishwa Vidyapeetham. Efficient charging of battery and production of power from solar energy, *In: Proceedings of the international conference on embedded systems* (ICES 2014). p. 231-237

[6] S. Gada, A. Fekik and All, Improving power quality in Grid-Connected Photovoltaic Systems: A Comparative Analysis of Model Predictive Control in Three-Level and Two-Level Inverters, MDPI Sensors, (2023).

[7] Henchiri, A., Bahi, T., Khochemane, L. Performances of solar photovoltaic under different climatic conditions, CIMSI, Mecanical Deparment, Skikda University, 2017, Algeria.

[8] A.S Kumar, V.U. Reddy, Performance evaluation of PV panel configurations considering PSC's for PV standalone applications. *Journal Européen System Automatised* , Vol. 54, No. 6, pp. 847-852. 2021, https://doi.org/10.18280/jesa.540606.

[9] Raja Azad Kumar Mishra, Energy Management in Grid Connected Photovoltaic System , *International Journal of Engineering Research & Technology* (IJERT), ISSN: 2278-0181, Vol. 9 Issue 02, 2020

[10] 1Alok Kumar Singh1 , Rajesh Gupta, Converter Configurations for Battery Management and Power Control in Standalone Solar PV fed Cascaded Multilevel Inverter, *J. Electrical Systems* , 18-3, 391-405, 2022.

[11] A Lakhdara, T Bahi, A Moussaoui , Study and Management of an Hybrid System Connected to The Network, *Journal of Electrical Systems JES*, Vol.18, N° 2, Pages 163-172, 2022.

[12] Kadeval, H. N., Patel, V. K. Mathematical modelling for solar cell, panel and array for photovoltaic system, in India, 937 – 943. 2021.

[13] S. Kolsi, H. Samet, M. Ben Amar, Design Analysis of DC-DC Converters Connected to a Photovoltaic Generator and Controlled by MPPT for Optimal Energy Transfer throughout a Clear Day, *Journal of Power and Energy Engineering,* Vol.2 No.1, 2014.

[14] Nguyen, X.H., Nguyen, M.P. Mathematical modelling of photovoltaic cell/module/arrays with tags in Matlab/Simulink. Environ Syst Res 4, 24 , 2015, . https://doi.org/10.1186/s40068-015-0047-9

[15] Ravi Prakash, Sandeep Singh, Designing and Modelling of Solar Photovoltaic Cell and Array, *Journal of Electrical and Electronics Engineering* (IOSR-JEEE) e-ISSN: 2278-1676,p-ISSN: 2320-3331, Vol.11, Issue 2 , 35-40, 2016.

[16] J. Surya Kumari, Ch. Sai Babu, Mathematical Modeling and Simulation of Photovoltaic Cell using Matlab-Simulink Environment , International Journal of Electrical and Computer Engineering (IJECE) Vol. 2, N°. 1, 26~34 , 2012, ISSN: 2088-8708

[17] A. Henchiri, T. Bahi, L. Khochemane, S. Lekhchine, Control of the DC Voltage Output Photovoltaic System, *5th International Conference on Green Energy and Environmental Engineering*, 28-30, 2018, Tunisia.

[18] Sathish Ch , Chidambaram Ia , Manikandan M , Switched Z-Source Boost Converter in Hybrid Renewable Energy System for Grid-Tied Applications, *J. Electrical Systems JES* 19-1 , 64-81., 2023.

[19] M. Rasheed, S. Shihab, Modelling and parameter extraction of PV cell using Single-Diode model. *Advanced energy conversion materials*, 96- 104. 2020, https://doi.org/10.37256/aecm.122020550.

[20] Santos, L.J.L., Antunes, F., Chehab, A., et al.: 'A maximum power pointtracker for PV systems using a high performance boost converter', Sol.Energy, 80, (7),pp. 772–778, 2006.

[21] Sathish C.H., Chidambaram I.A., Manikandan M.Switched Z-Source Boost Converter in Hybrid Renewable Energy System for Grid-Tied Applications, Journal of Electrical System , Vol 19 N°1 Vol. 19 No. 1 , 2023.

[22] Reza Dowlatabadi , Mohammad Monfared, Saeed Golestan, Amir Hassanzadeh, Modelling and Controller Design for a Non-inverting Buck-Boost Chopper, *International Conference on Electrical Engineering and Informatics*, 17-19 July 2011, Bandung, Indonesia

[23] Birane M., Derrouazin A., Aillerie M., Cheknane A., Larbes C.? Evaluation and performance of different topologies of converters with efficient MPPT in a photovoltaic system, Journal of Electrical System, JES Vol. 16 No. 3, 2020.

[24] A. Soetedjo, Y. I. Nakhoda and C. Saleh, imulation of Fuzzy Logic Based Energy Management for the Home with Grid Connected PV-Battery System, *2nd International Conference on Smart Grid and Smart Cities (ICSGSC)*, Kuala Lumpur, Malaysia, pp. 122-126, 2018, doi: 10.1109/ICSGSC.2018.8541271.
[25] Baqar, A.; Camara, M.B.; Dakyo, B. Energy Management in the Multi-Source Systems. *Energies* 2, *15*, https://doi.org/10.3390/en15082713.
[26] J. -A. V. Magsumbol et al., "FLi-BMS: A Fuzzy Logic-based Intelligent Battery Management System for Smart Farm, *IEEE 14th International Conference on Humanoid, Nanotechnology, Information Technology, Communication and Control, Environment, and Management (HNICEM),* Boracay Island, Philippines, pp. 1-5, 2022, , doi: 10.1109/HNICEM57413.2022.10109388.
[27] Subudhi, B.; Pradhan, R. A Comparative Study on Maximum Power Point Tracking Techniques for Photovoltaic Power Systems. *IEEE Trans. Sustain. Energy*, 4, 89–98, 2013.
[28] Mohammad Sarvi and Ahmad Azadian, A comprehensive review and classified comparison of MPPT algorithms in PV systems, Energy Systems, Vol. 13, 281 – 320, 2021.
[29] Khaled Bataineh, Improved hybrid algorithms-based MPPTalgorithm for PV system operating undersevere weather conditions, *IET Power Electronic, Vol. 12 Iss. 4, 703-7112019,*
[30] Wafa Hayder , Emanuele Ogliari , Alberto Dolara , Aycha Abid , Mouna Ben Hamed , Lasaad Sbita, Improved PSO: A Comparative Study in MPPT Algorithm for PV System Control under Partial Shading Conditions, *Energies*, MDPI, vol. 13(8), 1-22, 2020.
[31] A. Alankrita, N. Pati, S.K. Adhikary, B. Mishra, Fuzzy logic based energy management for grid connected hybrid PV system, Energy Reports, Vol. 8, Supplement 10, 751-758, 2022, ISSN 2352-4847, https://doi.org/10.1016/j.egyr.2022.05.217.
[32] Unal Yilmaz, Ali Kircay, Selim Borekci,, PV system fuzzy logic MPPT method and PI control as a charge controller, *Renewable and Sustainable Energy Reviews*,Vol. 1, Part 1, 994-1001, 2018, ISSN 1364-0321,https://doi.org/10.1016/j.rser.2017.08.048.